



OPEN ACCESS

EDITED BY

Agustin Sanchez-Arcilla,
Universitat Politecnica de Catalunya, Spain

REVIEWED BY

Angelo Fraga Bernardino,
Federal University of Espirito Santo, Brazil
Cibele Amaral,
University of Colorado Boulder, United States

*CORRESPONDENCE

Juan Fernando Gallardo Lancho
✉ juanf.gallardo@gmail.com
Claudia Maricusa Agraz Hernández
✉ clmagraz@uacam.mx

RECEIVED 11 October 2025

REVISED 11 December 2025

ACCEPTED 19 December 2025

PUBLISHED 23 January 2026


CITATION

Chávez-Barrera JC, Gallardo Lancho JF, Osti-Sáenz J, Gallegos Martínez ME, Ruiz-Fernández AC, Puschendorf R and Agraz Hernández CM (2026) Restoration enhances carbon storage in mangroves after hurricane impacts. *Front. Mar. Sci.* 12:1722651. doi: 10.3389/fmars.2025.1722651

COPYRIGHT

© 2026 Chávez-Barrera, Gallardo Lancho, Osti-Sáenz, Gallegos Martínez, Ruiz-Fernández, Puschendorf and Agraz Hernández. This is an open-access article distributed under the terms of the [Creative Commons Attribution License \(CC BY\)](https://creativecommons.org/licenses/by/4.0/). The use, distribution or reproduction in other forums is permitted, provided the original author(s) and the copyright owner(s) are credited and that the original publication in this journal is cited, in accordance with accepted academic practice. No use, distribution or reproduction is permitted which does not comply with these terms.

Restoration enhances carbon storage in mangroves after hurricane impacts

Julio César Chávez-Barrera¹, Juan Fernando Gallardo Lancho ^{2*}, Juan Osti-Sáenz³, Margarita Elizabeth Gallegos Martínez⁴, Ana Carolina Ruiz-Fernández⁵, Robert Puschendorf⁶ and Claudia Maricusa Agraz Hernández^{3*}

¹Doctorado en Ciencias Biológicas y de la Salud, Universidad Autónoma Metropolitana, Ciudad de México, Mexico, ²Retired, Salamanca, Spain, ³Instituto de Ecología, Pesquerías y Oceanografía del Golfo de México, Universidad Autónoma de Campeche, Campeche, Mexico, ⁴Departamento de Hidrobiología, Unidad Iztapalapa, Universidad Autónoma Metropolitana, Ciudad de México, Mexico, ⁵Instituto de Ciencias del Mar y Limnología, Unidad Académica Mazatlán, Universidad Nacional Autónoma de México, Sinaloa, Mexico, ⁶School of Biological and Marine Sciences, University of Plymouth, Plymouth, United Kingdom

Mangroves are globally important blue-carbon ecosystems, yet their resilience is threatened by extreme weather events and hydrological alterations. In southeastern Mexico, a large mangrove die-off occurred in 1995 following Hurricane Roxanne and Tropical Storm Opal, linked to storm-surge-driven hypersalinity, sedimentation, and prolonged flooding. In 2005, an ecological restoration program was launched in the Términos Lagoon region, focusing on hydrological rehabilitation and reforestation with *Avicennia germinans*. Fourteen years later, we assessed ecosystem recovery by quantifying total ecosystem carbon stocks (TECS), defined as the sum of 0–50-cm soil organic carbon and tree biomass carbon, across conserved, degraded, and restored sites, and by reconstructing vegetation cover dynamics from multi-decadal satellite imagery (1984–2023). TECS differed markedly among conditions: The restored site accumulated $286.0 \pm 32.6 \text{ Mg C ha}^{-1}$ (83% of the conserved site), whereas degraded sites stored only $133.0 \pm 26.8 \text{ Mg C ha}^{-1}$. The increase in TECS at the restored site was primarily associated with enhanced soil organic carbon stocks, consistent with improved hydroperiod, recovery of interstitial water physicochemical conditions, and renewed autochthonous organic matter inputs following hydrological reconnection and initial reforestation. Biomass carbon remained lower at the restored site, reflecting younger stand age, although vegetation indices indicated rapid canopy recovery within 7 years of the intervention. These results show that hydrological rehabilitation can substantially reestablish long-term carbon storage capacity in hurricane-impacted mangroves and highlight the need for sustained monitoring to evaluate ecosystem service recovery and guide climate mitigation and coastal resilience strategies.

KEYWORDS

blue carbon, Campeche State, Hurricane Roxanne, hydrological rehabilitation, mangroves

1 Introduction

Mangroves act as natural coastal barriers, protecting shorelines from storms while supporting biodiversity across both marine and terrestrial ecosystems (Getzner and Islam, 2020). They also play a critical role in climate change mitigation, as they efficiently sequester and store atmospheric carbon (Donato et al., 2011; Troche-Souza et al., 2025). Despite these benefits, mangroves are experiencing rapid global decline due to anthropogenic pressures and environmental change (Alongi, 2020). In Mexico, the Yucatán Peninsula hosts the country's largest mangrove area, yet it faces accelerating habitat loss (Agraz-Hernández et al., 2020). Degradation is particularly severe within the Términos Lagoon Flora and Fauna Protection Area (TLFFPA), which contains the nation's largest saline coastal lagoon. This protected area is not only of outstanding ecological value but also of economic importance, as it overlaps with major oil extraction activities and supports key local fisheries (Grenz et al., 2017). Mangrove forests in this region are under chronic stress from altered hydrological regimes, eutrophication, and pollution associated with urban expansion, agriculture, and municipal wastewater discharges, leading to large-scale mortality events (Macías Samano et al., 2025). Moreover, the high frequency of hurricanes in the region further exacerbates ecosystem vulnerability (Rivera-Monroy et al., 2020; Amaral et al., 2023). Tropical cyclones can cause significant short-term damage to mangrove forests, including defoliation and tree tilting from intense winds, although these impacts are often reversible within a few months (Xiong et al., 2022). In contrast, severe hurricanes can trigger large-scale mangrove die-offs through storm surges that result in prolonged flooding, hypersalinity, and hypoxic conditions, all of which severely impair ecosystem function and recovery (Lagomasino et al., 2021).

In terms of carbon (C) storage, available evidence suggests that the recovery of pre-disturbance C stocks depends strongly on hurricane intensity, underscoring the importance of early identification of areas requiring restoration. For example, Griffiths and Mitsch (2021) reported that, following a Category 3 hurricane in Florida, soil organic carbon (SOC) stocks in the surface layer (0–20 cm) decreased due to mangrove mortality and oxidation of peaty SOC, even though vegetation structure and aboveground biomass recovered relatively quickly. In contrast, Peneva-Reed et al. (2021) documented that, after a more intense Category 5 hurricane, most affected mangrove areas remained without vegetation and showed estimated carbon losses of 427–3,599 Mg C ha⁻¹, which did not return to pre-event levels. Such severe disturbances can therefore cause substantial C losses, reducing the capacity of mangroves to function as carbon sinks while simultaneously contributing to atmospheric CO₂ emissions and disrupting nutrient cycling.

Restoration initiatives are therefore increasingly implemented to counteract storm-driven degradation, with the goal of enhancing C storage and improving the resilience of coastal ecosystems in the face of more frequent and intense climatic disturbances (Coumou and Rahmstorf, 2012). However, restoration outcomes depend critically on reestablishing favorable hydroperiods and environmental conditions that allow mangrove propagules and

seedlings to survive and grow, which remains one of the most challenging aspects of large-scale restoration projects (Lewis, 2005; Krauss et al., 2008).

Restoration of impacted mangrove forests through hydrological rehabilitation (HR) has been identified as an effective strategy for ecosystem recovery, particularly in sites where alterations to water flow patterns hinder natural regeneration (Lewis, 2005; Agraz Hernández et al., 2024). This is the case in our study area (Laguna de Términos, Campeche State, Mexico), where Hurricane Roxanne caused intense sediment deposition that blocked natural tidal channels, altered the hydroperiod, increased interstitial salinity, and generated prolonged hypoxic conditions (Agraz Hernández et al., 2015). These hydrological disruptions exceeded the physiological thresholds required for propagule establishment and seedling survival, thereby preventing natural recovery. In this context, HR typically involves removing blockages in natural channels and excavating artificial ones to reestablish the hydroperiod, the frequency, duration, and depth of tidal flooding—while also restoring freshwater inputs to the affected area (Agraz Hernández et al., 2015). By recreating these hydrological conditions, HR addresses one of the primary barriers to mangrove survival and sets the stage for long-term ecological recovery.

In the short term, these actions stimulate natural regeneration processes, enhance the survival of reimplanted seedlings, and improve soil properties (≤ 4 years; Chávez Barrera et al., 2025). Beyond ecological outcomes, HR also generates socioeconomic benefits for local communities. Activities such as channel dredging, monitoring, and planting provide paid employment opportunities and strengthen community engagement. In some regions of Mexico, including areas with Mayan communities, these restoration activities receive financial support from government institutions in collaboration with local universities, which design large-scale projects and manage the associated resources. This scheme functions as a structured, long-term employment mechanism that enables community participation in mangrove restoration and represents a distinctive local model compared with most restoration initiatives globally (Laboratorio de Humedales Costeros, 2025).

Nevertheless, large-scale mangrove restoration projects face considerable challenges, in part due to the scarcity of long-term monitoring data from successful efforts and the limited number of projects that report outcomes in a comparable way (Gerona-Daga and Salmo, 2022; Gatt et al., 2024). The Mangrove Restoration Tracker Tool, for example, shows that relatively few initiatives provide robust information on ecological and social performance, highlighting gaps in funding, capacity, and standardized indicators for evaluating progress (Gatt et al., 2024). The failure of numerous mangrove restoration projects is also linked to an insufficient understanding of degradation drivers, which limits the appropriate selection of recovery strategies (Hai et al., 2020). Low survival rates are often due to inappropriate species choice or reforestation under environmental conditions outside mangrove tolerance thresholds (Lewis, 2005), whereas low community participation, associated with a lack of incentives and local organization, reduces the continuity of management (Lovelock et al., 2022). Because each community values ecosystem services differently, their degree of involvement in restoration also varies (Owuor et al., 2024). Overall,

the evidence shows that the most successful projects are those in which the local community takes ownership of the process and establishes long-term sustainable management mechanisms, as documented in Benin through hydrological rehabilitation and control of invasive grasses (Agraz-Hernández et al., 2025). Even in countries such as Mexico, which leads Latin America in mangrove restoration investment (Grimm et al., 2023), information on ecosystem recovery, particularly the recovery of carbon sequestration services, remains limited. Generating robust data on carbon capture capacity can incentivize governments to restore degraded mangroves, reinforcing environmental commitments and reducing greenhouse gas emissions. Therefore, it is important to determine whether, and on what timescale, restored mangroves can store carbon as efficiently as pristine forests (Bourgeois et al., 2024). In addition, quantifying carbon stock recovery helps refine ecological restoration strategies, while also providing private initiatives with a basis for evaluating returns on investment in carbon credit projects (Duncan et al., 2022).

In this study, we assess the impacts of hurricane-driven degradation on the carbon storage capacity of mangroves in the Términos Lagoon Flora and Fauna Protection Area (Campeche, Mexico). We hypothesize that hydrological rehabilitation, combined with reforestation with *Avicennia germinans*, enhances the recovery of soil carbon storage and drives restored sites toward levels comparable with conserved stands. To test this hypothesis, we compared total ecosystem carbon stocks, including aboveground and belowground carbon from biomass and soil, across three sites: conserved, degraded, and restored. Complementary analyses of pore water and soil physicochemical properties, together with vegetation dynamics reconstructed from multi-decadal NDVI time series, provided additional insights into the drivers of degradation and the performance of restoration activities in promoting ecosystem resilience and service recovery.

In this study, we aim to assess whether ecological restoration can recover carbon stocks in hurricane-impacted mangroves and over what time frame. To this end, we first analyzed changes in mangrove canopy cover using remotely sensed normalized difference vegetation index (NDVI) time series to reconstruct historical variations and link hurricane-induced mortality with post-restoration recovery. We then compared soil physicochemical properties and carbon pools among three conditions—restored, degraded, and conserved sites—to evaluate differences in total ecosystem carbon stocks.

2 Materials and methods

2.1 Study area

Mexico ranks fourth globally in mangrove area (Bunting et al., 2018), and the state of Campeche in southern Mexico contains the country's second-largest mangrove extent (Velázquez-Salazar et al., 2020). In Campeche, mangroves are mainly concentrated in the Los Petenes Biosphere Reserve (20°31'–19°49' N, 90°45'–90°20' W) and in the Términos Lagoon Flora and Fauna Protection Area (TLFFPA; 18°40' N, 91°45' W) (Agraz-Hernández et al., 2020).

Despite their importance, mangroves in Campeche, and particularly those within the TLFFPA, have been subjected to severe and recurrent degradation driven by urban expansion, eutrophication, hydrological alterations, droughts, and tropical cyclones (Agraz-Hernández et al., 2022). The region is characterized by persistent tropical cyclone activity. Records from 1970 to 2020 show a continuous occurrence of tropical depressions with a marked increase in frequency after 1999 (Supplementary Figure S1). Tropical storms also increased steadily from 1995 onward, becoming the most common cyclone type. Category 1 hurricanes (Saffir–Simpson scale) occurred most frequently, whereas more intense events (Categories 3–5) were recorded sporadically in 1974, 1975, 1979, 1980, 1989, 1995, 2002, 2005, and 2007. The 1995 season was particularly severe, marked by Hurricane Roxanne and Tropical Storm Opal. Data from the NOAA interactive platform indicate that Hurricane Roxanne intensified rapidly and followed an unusual trajectory, briefly reentering the Gulf of Mexico before making a second landfall (Supplementary Figure S2). Consistent with these meteorological events, several studies have documented mangrove mortality within the TLFFPA, including areas near our study site (Echeverría-Ávila et al., 2019).

In response to this degradation, the Coastal Wetlands Laboratory at the Institute for Ecology, Fisheries, and Oceanography of the Gulf of Mexico (EPOMEX) initiated a large-scale restoration project in 2005. The project targeted a 104.5-ha degraded mangrove area within the TLFFPA, with the aim of restoring ecological health through hydrological rehabilitation (HR) (Figure 1). The HR program was designed using detailed microtopographic mapping of the degraded site, which revealed zones with elevated salinity and oxygen deficits (Agraz-Hernández et al., 2015). To restore hydrological connectivity, we excavated a network of artificial channels, including a primary channel 2 m wide, 1.5 m deep, and 1 km long, interconnected with 15 secondary hand-dug channels (1 × 1 m) that improved water movement and landscape connectivity (Figures 1c, d). In addition, natural tidal channels that had been blocked by hurricane-deposited sediments were dredged to reestablish tidal exchange and freshwater inflows (Figure 1b). Through these interventions, we sought to recover the natural hydroperiod and reestablish soil and water physicochemical conditions within the tolerance ranges observed in reference mangrove stands dominated by *Avicennia germinans* and *Rhizophora mangle*.

Reforestation was initiated once pore-water salinity and redox potential reached values comparable with those of the conserved site. Of the 104.5-ha intervention area, 17.5 ha was actively reforested in zones where microtopography and hydroperiod supported seedling establishment, whereas the remaining area was left to regenerate naturally under improved hydrological conditions. Nursery-grown *Avicennia germinans* seedlings were planted within the reforested plots (Figures 1e, f), and *Rhizophora mangle* propagules were directly established along channel banks to stabilize sediments and reduce erosion. Local communities played a central role in these activities, maintaining channels and contributing to the long-term success of hydrological rehabilitation.

For this study, we designated the 17.5-ha reforested section as the restored site (Mres; 18°42.676' N, 91°36.561' W; Figure 1).

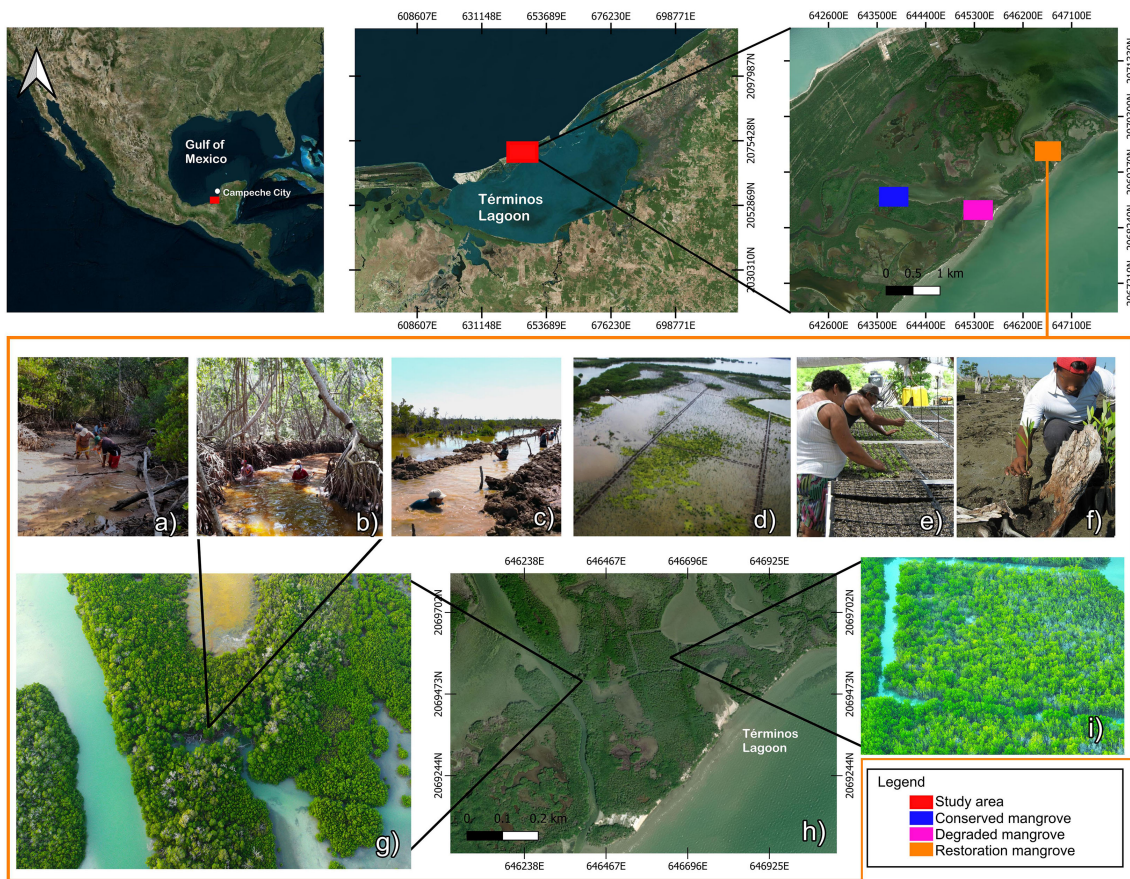


FIGURE 1

Study area within the Términos Lagoon Flora and Fauna protection area (Campeche State, Mexico), showing the conserved, restored, and degraded mangrove sites. (a–c) Local Mayan community members manually cleaning and dredging natural channels as part of initial hydrological rehabilitation efforts in 2005. (a) Natural channel prior to dredging, showing sediment accumulation and obstructed water flow. (b) Natural channels after dredging, with water flow restored. (c, d) Excavation of artificial channels within the restored site. (e, f) Reforestation efforts using *Avicennia germinans* and *Rhizophora mangle*. (g) Drone image of dredged natural channels connected to the restored site and estuary. (h) Aerial view of the restored site in 2019. (i) Drone image showing vegetation recovery 14 years after reforestation with *A. germinans*.

We selected a nearby degraded site without intervention as a comparison (18°42.163' N, 91°37.316' W) and identified a conserved mangrove forest that met the Society for Ecological Restoration (SER) criteria as the conserved site (18°42.462' N, 91°38.451' W). This conserved site served as the benchmark for assessing restoration outcomes, representing the structural and functional attributes of a healthy mangrove ecosystem. Although the sites are slightly separated geographically, they lie within the same environmental unit and share comparable conditions, as characterized by previous studies (Agraz Hernández et al., 2015). Similarities in hydrology, salinity, and vegetation structure support the comparability of the restored, degraded, and conserved sites for evaluating restoration outcomes.

2.2 Field data collection

At each study site (conserved, degraded, and restored), we established three permanent square plots of 10 × 10 m (100 m²), separated from each other by 20 m. This design followed the general

guidelines of Kauffman and Donato (2012) but was adapted to our restoration context and long-term monitoring objectives. In particular, the size, number, and square shape of the plots were defined based on protocols applied in mangroves under restoration (Agraz Hernández et al., 2024; Chávez Barrera et al., 2025) and on logistical constraints associated with repeated measurements. Permanent square plots marked at the corners facilitate precise relocation in future campaigns, as these same plots are being used in a parallel long-term study at the three sites. We acknowledge that the number of plots per site is lower than in the original Kauffman and Donato protocol and consider this a limitation when interpreting within-site variability. In each plot, we measured trunk diameter and height to estimate carbon stored in tree biomass following standardized methods (Kauffman and Donato, 2012) and collected soil cores to analyze redox potential and soil organic carbon (SOC) content. All measurements were conducted in 2019.

Because baseline (“zero-time”) carbon data were unavailable at the restored site, we used a nearby mangrove stand within the TLFPPA as a proxy for pre-restoration conditions. This stand was

impacted by the 1995 cyclone season (Tropical Storm Opal and Hurricane Roxanne; Echeverría-Ávila et al., 2019), has not undergone any restoration, and was classified as degraded (Mdeg) based on 2019 field observations of extensive canopy loss, predominance of dead trees, storm-deposited sediments and shells, blocked tidal channels, hypersaline pore water, and lack of natural regeneration (Supplementary Figure S3).

2.3 Remote sensing analysis of mangrove vegetation cover before and after restoration

To reconstruct long-term vegetation cover dynamics, we calculated the Normalized Difference Vegetation Index (NDVI) for the restored site over a 39-year period (November 1984–February 2023) and compared it with the conserved site. NDVI values range from -1 to 1 , with values closer to 1 indicating dense, healthy vegetation and values near -1 indicating sparse or absent vegetation. By analyzing temporal variations in NDVI, we identified the decline in canopy cover associated with the 1995 cyclone season (Tropical Storm Opal and Hurricane Roxanne) and evaluated subsequent ecosystem recovery following hydrological rehabilitation and reforestation. NDVI has been widely applied in mangrove restoration research (Tran et al., 2022; Winarso et al., 2023).

We obtained NDVI values from Google Earth Engine by combining the red and near-infrared (NIR) spectral bands of Landsat 5, Landsat 7, and Landsat 8 imagery. To minimize noise from outliers and cloud cover, we applied the Savitzky–Golay smoothing technique (Chen et al., 2004) and then calculated yearly median NDVI values for each site from the processed satellite images.

2.4 Pore water parameters

To determine pore water parameters, we constructed piezometers (gravity water collectors) from PVC tubes 10.16 cm in diameter and 1.50 m in length (Agraz-Hernández et al., 2022). We perforated the lower 30 cm of each tube with 1.0-cm holes to allow pore-water entry and to minimize sample oxidation or alteration of natural chemical composition. After installing the piezometers, we manually drained the contained water using a small PVC extractor tube connected to a recipient. Once the water level stabilized, we measured redox potential *in situ* with a multiparameter probe (Hach HQ40D), expressed in millivolts (mV). We then extracted pore-water samples with the PVC extractor and measured salinity using a refractometer (A&O, range: 0–100 PSU) (Agraz-Hernández et al., 2022).

We carried out measurements at all study sites (conserved, degraded, and restored) twice during 2019: once in the dry season (March) and once in the rainy season (July). For the restored site, we also analyzed a historical database of pore-water salinity provided by the Coastal Wetlands Laboratory of the EPOMEX Institute (n.d.). This dataset included monthly records from 2005 (pre-restoration)

through 2010 (post-restoration), which enabled us to evaluate changes in pore-water physicochemical conditions and hydroperiod recovery over six consecutive years following restoration.

2.5 Soil organic carbon content and redox potential

At each site (conserved, degraded, and restored), we collected three soil cores (one per plot), initially aiming for a depth of 1.0 m. However, highly compacted layers, particularly at the degraded site, prevented deeper sampling, so SOC analyses were standardized to 0–50 cm at all sites, which we acknowledge as a limitation. Cores were extracted using 6.35-cm-diameter PVC tubes fitted with a semi-cylindrical insert to maintain core integrity and a carefully sharpened, serrated lower edge to cut through compacted sediment and roots (Chávez-Barrera et al., 2025). During sampling, the tubes were inserted slowly with a clockwise rotational motion to reduce compaction and avoid altering bulk density; once the target depth was reached, a tight lid was placed on top to create a vacuum and prevent core disturbance during extraction.

After recording redox potential, we sectioned the cores at 5-cm intervals, sealed the samples in airtight plastic bags, and transported them to the laboratory. We lyophilized the samples for 4 days and recorded dry weight to calculate bulk density. We then manually homogenized the material and obtained a 10-g subsample. Each subsample was pulverized with a TissueLyser II (Qiagen GmbH, Hilden, Germany) to standardize particle size and improve precision in soil organic carbon (SOC) analysis. From the pulverized material, we weighed a 5.0-mg subsample into silver capsules using a Mettler Toledo XP6 microbalance (standard deviation: $\pm 1 \mu\text{g}$). We pretreated the samples with 6.15 M hydrochloric acid to remove inorganic carbon. We determined SOC concentration (%) by dry combustion with a Flash 2000 elemental analyzer (Thermo Fisher Sci. Inc., Waltham, MA, USA), calibrated with certified standards, at the Coastal Wetlands and Gas Emissions Laboratory of the EPOMEX Institute, following the method described by Chávez Barrera et al. (2025).

To calculate total soil carbon (Mg C ha^{-1}), we applied Equation 1 to each depth interval and summed the values to obtain SOC content to a 50-cm depth (Kauffman and Donato, 2012):

$$\begin{aligned} \text{SOC } (\text{Mg C ha}^{-1}) \\ = \text{Bulk density } (\text{g cm}^{-3}) \times \text{SOC } (\%) \times \text{Depth } (\text{cm}) \quad (1) \end{aligned}$$

We calculated bulk density by dividing the dry weight of the lyophilized soil by sample volume, using the corer diameter and a 5-cm sampling depth per segment for volume determination.

2.6 Organic carbon in tree biomass

We estimated aboveground and belowground biomass of living and dead standing trees using published allometric equations.

Biomass carbon was expressed on a dry-matter basis. To estimate aboveground biomass for *Avicennia germinans*, we applied species-specific equations. For the restored forest, we used the equation developed by Day et al. (1987), which was derived near the study area and is suited for trees with diameters between 0 and 10 cm, matching those observed at this site. For the conserved and degraded sites, we applied the equation by Fromard et al. (1998), designed for larger diameters and developed for mangroves in French Guiana. Both models, based on sample sizes of 20–25 trees, showed a strong relationship between biomass and diameter ($R^2 = 0.97$), confirming the reliability of aboveground biomass estimates. Because species-specific models for belowground biomass of *A. germinans* are limited, we used the general allometric equation proposed by Komiyama et al. (2008).

We applied the same allometric equations used for living trees to estimate the biomass of standing dead trees, incorporating corrections based on their decomposition stage as recommended by Kauffman and Donato (2012). We then converted aboveground and belowground biomass of both living and dead trees to carbon using conversion factors of 0.48 and 0.39, respectively (Kauffman and Donato, 2012). Finally, we calculated total carbon content in tree biomass as the sum of these components and expressed the results in megagrams of carbon per hectare (Mg C ha^{-1}).

2.7 Total ecosystem carbon stock

We calculated total ecosystem carbon stock (TECS) at each study site by summing carbon stored in tree biomass and soil organic carbon (SOC) to a depth of 50 cm, expressed in Mg C ha^{-1} . For each site, TECS was obtained from the mean of all plots within that condition. To evaluate the effectiveness of ecological restoration in reestablishing mangrove carbon storage, we expressed TECS at the restored site as a percentage of TECS at the conserved site, indicating the proportion of carbon recovered relative to a conserved mangrove.

2.8 Statistical analysis

To assess environmental changes resulting from hydrological rehabilitation, we performed a one-way analysis of variance (ANOVA) on pore-water salinity concentrations from the year before restoration (2005) and the following years (2006–2010). Fourteen years after restoration, we used one-way ANOVA to compare soil and pore-water physicochemical properties, tree biomass recovery, basal area, tree density, and carbon storage across degraded, restored, and conserved sites. We tested variable normality with the Shapiro–Wilk test (1965) and applied Fisher's least significant difference (LSD) test for *post-hoc* comparisons.

We evaluated relationships between soil bulk density, redox potential, and SOC content using linear regression. To analyze vegetation dynamics, we examined changes in the normalized difference vegetation index (NDVI) before, during, and after restoration using linear models. We carried out all statistical

analyses in Minitab 19.1, applying a significance threshold of $\alpha = 0.05$.

3 Results

3.1 Remote sensing analysis of mangrove vegetation cover before and after restoration

NDVI analysis of the restored site (Mres) revealed a sharp mortality event in 1996, with a 60.47% decrease compared with 1995 (NDVI = 0.175), likely associated with the Hurricane Roxanne and Tropical Storm Opal occurred during this year (Figure 2). Prior to restoration, NDVI values showed a steep decline from 0.73 in 1984 to 0.23 in 2004. This reduction occurred in two phases: from 1984 to 1994, NDVI decreased at an annual rate of -0.024 ($R^2 = 0.93$); from 1997 to 2004, values remained consistently low until restoration began in 2005.

Following restoration, NDVI rose from 0.28 in 2005 to 0.78 in 2011, increasing at an annual rate of 0.095 ($R^2 = 0.955$). By the seventh year after intervention, NDVI stabilized and remained steady during 2022, approaching the levels observed at the conserved site but not reaching them (Figure 2).

3.2 Mangrove forest structure and physicochemical traits of the pore water

Across the three site conditions (conserved, degraded, and restored), *Avicennia germinans* was the dominant species. The conserved site had a mean basal area of $28 \pm 2 \text{ m}^2 \text{ ha}^{-1}$, whereas the restored site had $10 \pm 1 \text{ m}^2 \text{ ha}^{-1}$, showing significant differences between sites ($F_{34} = 154.44$, $p < 0.0001$; Table 1). Tree density also varied significantly among sites (Table 1). Tree biomass at the conserved site was 56% higher than at the restored site ($F_{34} = 24.32$; $p < 0.01$; Table 1). Mortality remained below 5% in both the conserved and restored sites, whereas the degraded site experienced 100% mortality and negligible tree biomass (Table 1).

Before hydrological rehabilitation in 2005, the restored site exhibited high pore-water salinity ($86 \pm 5 \text{ PSU}$; $F_{2475} = 12.29$, $p < 0.0001$; Supplementary Figure S4). Within 1 year of intervention, salinity declined to $59 \pm 17 \text{ PSU}$ at the restored site, with significantly lower values recorded in 2006 ($F_{2475} = 28.63$, $p < 0.0001$). This decreasing trend continued, and salinity stabilized from 2007 to 2010 (Supplementary Figure S4).

Fourteen years after restoration, the restored site maintained low-salinity conditions, as shown by 2019 measurements. Salinity remained in the mesohaline range at the restored site ($34 \pm 12 \text{ PSU}$), significantly lower than at the degraded site ($71 \pm 6 \text{ PSU}$; $F_{2,10} = 5.95$, $p = 0.02$; Figure 3). Pore-water redox potential also indicated less reducing conditions in 2019, with significantly higher oxygen availability at the restored site ($-313 \pm 28 \text{ mV}$; $F_{2,10} = 5.0$, $p = 0.031$; Figure 3). Overall, salinity and redox potential at the restored site converged toward the conditions observed at the conserved site (44 PSU and -313 mV), as confirmed by *post-hoc* analysis (Figure 3).

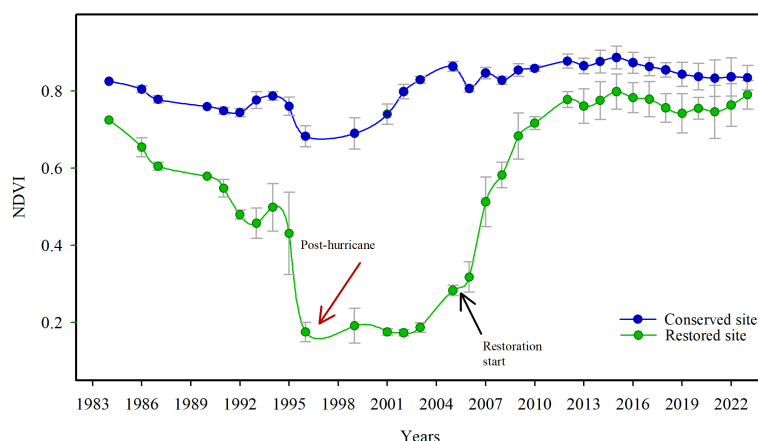


FIGURE 2

Normalized difference vegetation index (NDVI) time series over 39 years at a restored mangrove site within the Términos Lagoon Flora and Fauna protection area (Campeche, Mexico), compared with a conserved mangrove. Red arrow indicates the NDVI value in 1996 (post-hurricane) in areas currently under restoration, as well as the black arrow indicates vegetation state in the restoration start (2005). Dots represent the annual median NDVI values, with vertical lines indicating the standard error.

3.3 Soil carbon storage and redox dynamics in degraded and restored mangroves

Soil organic carbon (SOC) to 50 cm depth was 199 ± 64 Mg C ha⁻¹ at the conserved site, 133 ± 27 Mg C ha⁻¹ at the degraded site, and 222 ± 30.7 Mg C ha⁻¹ at the restored site. Differences among sites were significant ($F_{2,77} = 6.23$, $p < 0.001$). At the conserved site, SOC was highest at the surface, with 47.77 Mg C ha⁻¹ in the 0–5 cm layer, and decreased gradually with depth to 10.22 Mg C ha⁻¹ at 45–50 cm. At the degraded site, SOC started at 13.31 Mg C ha⁻¹ at 0–5 cm, increased slightly to 15.98 Mg C ha⁻¹ at 10–15 cm and reached a maximum of 22.22 Mg C ha⁻¹ at 15–20 cm, then declined to 7.05 Mg C ha⁻¹ at 45–50 cm, showing a more irregular pattern than at the conserved site. At the restored site, SOC accumulated mainly in the upper 15 cm, with a maximum of 31.60 Mg C ha⁻¹, whereas the lowest values were observed at 40–45 cm (11.85 Mg C ha⁻¹). Overall, SOC decreased significantly with depth across the three sites ($R^2 = 0.52$, $p < 0.0001$; Figure 4).

Redox potential profiles also differed among sites. The mean redox potential was -219 mV at the conserved site and -398 mV at the degraded site, indicating generally more reducing conditions in the degraded mangroves. At the restored site, mean redox potential increased to -186 mV, and differences among sites were significant ($F_{2,37} = 7.74$, $p < 0.001$; Figure 4). Redox potential varied consistently with depth at all sites. In the conserved site, values were -8.45 mV at the surface (0–5 cm) and became progressively more reducing with depth, reaching -311.78 mV at 45–50 cm. In the degraded site, strongly reducing conditions were recorded from the surface (-382.07 mV at 0–5 cm), increasing moderately to -350.71 mV at 10–15 cm and -259.08 mV at 15–20 cm and then decreasing again to highly reducing values at 45–50 cm (-455.12 mV). In the restored site, the redox potential was -19.6 mV at the surface and reached a positive value at 10–15 cm (46.35 mV) and then fluctuated between

-39.4 and -32.6 mV at 15–20 cm. At greater depths, redox potential decreased again, reaching -383.1 mV at 35–40 cm, -387.8 mV at 40–45 cm, and -259.3 mV at 45–50 cm.

Bulk density also varied significantly among 5 cm intervals down to 50 cm depth ($F_{2,69} = 6.28$, $p < 0.0001$; Figure 4), increasing below 30 cm in a pattern that paralleled redox trends. At the conserved site, bulk density remained relatively stable in the upper 30 cm, ranging from 0.34 to 0.43 g cm⁻³, starting at 0.41 g cm⁻³ at 0–5 cm and increasing moderately in deeper layers, with 0.70 g cm⁻³ at 40–45 cm and 0.53 g cm⁻³ at 45–50 cm. At the degraded site, bulk density showed the strongest increase with depth, from 0.40 g cm⁻³ at the surface to more than 0.70 g cm⁻³ from 30 to 35 cm downward, with a maximum of 0.86 g cm⁻³ at 45–50 cm. At the restored site, bulk density was lowest in surface layers (0.25 g cm⁻³ at 0–5 cm) and remained low to 20 cm and then increased progressively with depth, reaching 0.36 g cm⁻³ at 30–35 cm and 0.44 – 0.46 g cm⁻³ between 40 and 50 cm, generally remaining below values recorded at the conserved and degraded sites. A strong positive relationship was detected between SOC and redox potential ($R^2 = 0.74$; $p < 0.05$; Supplementary Figure S5).

3.4 Carbon storage of the mangrove restored site compared with the conserved and degraded sites

The conserved site stored the highest total ecosystem carbon stock (TECS), averaging 345 ± 82 Mg C ha⁻¹ (Figure 5). The restored site followed, whereas the degraded site contained significantly lower TECS ($F_{2,5} = 6.97$, $p < 0.05$). TECS at the degraded site was 60% lower than at the conserved site. This reduction was driven mainly by the loss of carbon stored in trees, although soils retained a substantial SOC pool representing 38% of the conserved site's TECS (Figure 5).

TABLE 1 Forest attributes and tree biomass in a conserved, degraded and restored mangrove forest in the Términos Lagoon Flora and Fauna Protection Area in Campeche State (southern Mexico).

Sites	Diameter (cm)	Basal area (m ² ha ⁻¹)	Tree density (Tree ha ⁻¹)	Tree biomass (Mg ha ⁻¹)
Conserved	13.0 ± 2.0	28.0 ± 1.5	7,400.0 ± 131.0	294.0 ± 42.6
Degraded	10.0 ± 2.0	1.4 ± 0.08	14.7 ± 2.1	10.0 ± 4.3
Restored	10.0 ± 3.0	10.3 ± 0.5	6,400.0 ± 566.0	129.0 ± 3.8

The data represent means of measurements taken during 2019.

At the restored site, TECS recovered to 83% of the conserved forest's storage capacity (286 ± 32.6 Mg C ha⁻¹). SOC was the main carbon pool recovered, accounting for 77% of TECS (222 Mg C ha⁻¹) and closely matching the 198.48 Mg C ha⁻¹ observed at the conserved site (Figure 5). In contrast, tree biomass recovered to only 44% of conserved-site values, reaching 58 Mg C ha⁻¹ compared with 147 Mg C ha⁻¹ at the conserved site (Figure 5).

4 Discussion

4.1 Drivers of mangrove decline and carbon loss

At the restored site (Mres), NDVI trends prior to restoration showed a marked decline in vegetation cover and productivity between 1984 and 1994 (Figure 2). This reduction coincided with recurrent droughts in 1981, 1986, and 1987 across the Yucatán Peninsula, including the Términos Lagoon region (De La Barreda et al., 2020). Higher temperatures and reduced rainfall during these droughts likely increased pore-water salinity, stressing mangrove stands, limiting photosynthetic activity, and lowering primary productivity (Agraz-Hernández et al., 2022).

Between 1996 and 2004, NDVI values at Mres corresponded to bare soil or dead mangrove stands (Figure 2), consistent with patterns reported in other studies (e.g., Asbridge et al., 2019) and confirmed by field surveys conducted before restoration began in 2004. In contrast, NDVI values at the conserved site (Mcon) remained stable during this period, suggesting that recurrent droughts alone cannot explain the mortality observed at Mres.

The mortality event at the restored site occurred shortly before and during the 1995 cyclone season, when Tropical Storm Opal struck the region, followed a week later by Hurricane Roxanne (Supplementary Figure S1). Landsea et al. (1998) reported that 1995 was an exceptionally active hurricane season, associated with a transition to La Niña conditions. Hurricane Roxanne (Category 3) is among the most destructive cyclones in the history of the Yucatán Peninsula. After making landfall and moving into the Gulf of Mexico, it returned to the coast with greater intensity, striking near the study area (Supplementary Figure S2), indicating that these cyclones were the primary cause of site degradation (Figure 2). This interpretation is supported by records of substantial mangrove losses south of the TLFFPA associated with these hurricanes (Echeverría-Ávila et al., 2019). Extensive mangrove areas were also destroyed near Ciudad del Carmen (north of the TLFFPA), causing considerable coastal geomorphological changes, such as erosion and sediment accumulation in the estuaries near the study site (Palacio Prieto et al., 1999).

Comparisons of soil and pore-water physicochemical characteristics between the degraded and conserved sites indicate that redox potential was significantly more reducing (anoxic) at the degraded site (Figures 3), suggesting hydrological conditions characterized by prolonged water residence times and limited oxygen diffusion in both soil and water column. These conditions are at least partly linked to the obstruction of natural channels by sediment accumulation (likely transported and deposited during hurricanes), as documented during the 2005 field survey of the restoration area (Figure 1a). Sediment accumulation may have limited water entry at high tide and drainage at low tide, leading to hydrological isolation and prolonged flooding. Overflooding is recognized as one of the main factors contributing to mangrove mortality after hurricanes, as it

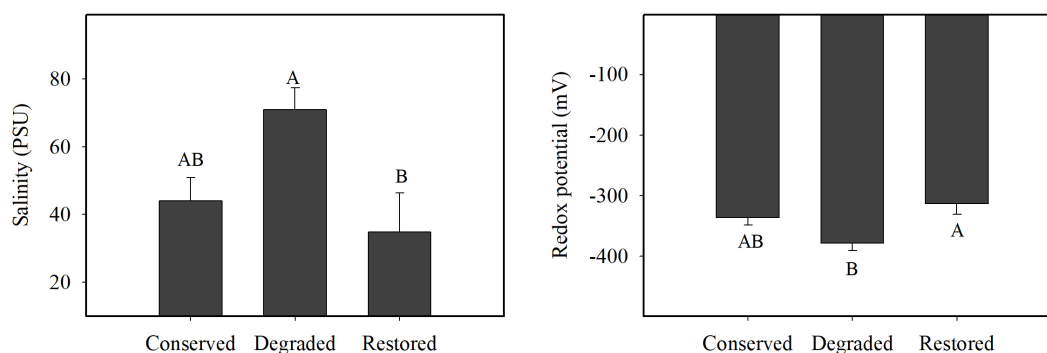


FIGURE 3

Trends in salinity and redox potential of pore water at three mangrove sites: conserved, degraded, and restored, within the Términos Lagoon Flora and Fauna protection area (Campeche, Mexico). Data represent mean values from two annual measurements conducted in 2019, 14 years after restoration. Vertical lines indicate the standard error of the mean. Different uppercase letters (A, B, C) denote statistically significant differences among sites, based on a *post-hoc* analysis.

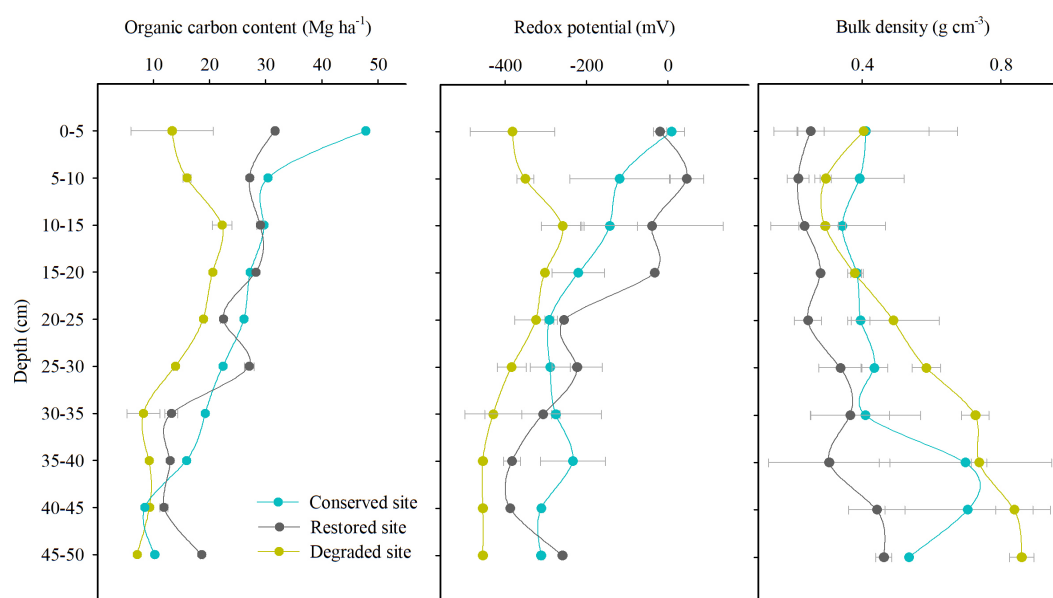


FIGURE 4

Soil organic carbon content, redox potential, and bulk density measured at -5 -cm intervals down to a depth of -50 cm in the conserved forest, degraded site, and restored site within the Términos Lagoon Flora and Fauna protection area (Campeche State, Mexico). Data represent mean measurements from 2019. Each point on the graph represents the mean value of each measured variable across three soil cores, with horizontal lines indicating the standard error of the mean.

increases oxygen deficit and favors the formation of phytotoxic compounds such as hydrogen sulfide (Lagomasino et al., 2021). It is likely that these anoxic conditions persisted at physiologically intolerable levels for the original mangrove species for nearly a decade after the hurricane impacts. This interpretation is supported by NDVI values, which remained within the characteristic range of dead mangroves or bare soil from 1996 to 2005 (Figure 2), indicating the absence of natural regeneration.

Without canopy recovery, prolonged exposure of the soil surface to direct solar radiation intensified evaporation and increased interstitial salinity, as observed at the degraded site, where hypersaline conditions were recorded (Figure 3). High salinity negatively affects mangrove physiological performance by increasing osmotic stress, reducing water uptake, decreasing photosynthetic capacity, and limiting survival (Pereira Silva et al., 2023), which in turn constrains the establishment of new seedlings. These environmental changes reduced the mangroves' carbon storage capacity by an estimated 60%, as reflected in the difference in TECS between the conserved and degraded sites. Widespread tree mortality caused a sharp decline in biomass carbon, and the absence of natural regeneration further limited carbon sequestration.

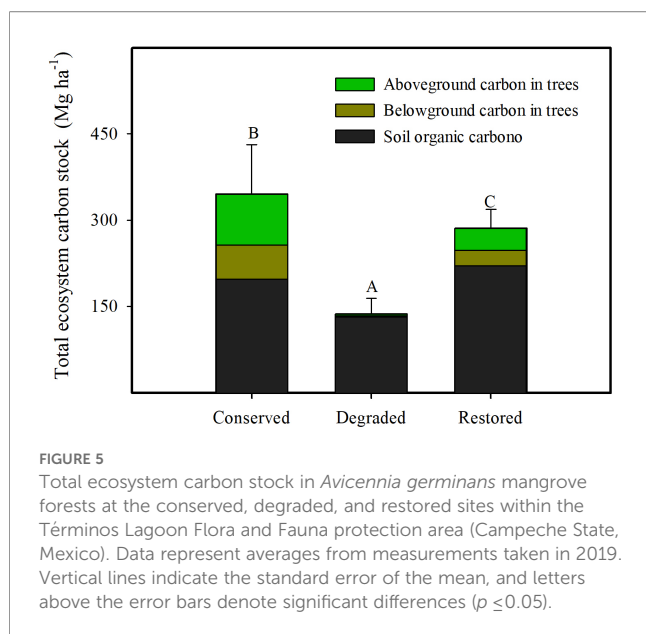
With respect to SOC, previous studies suggest that hurricane-driven mangrove mortality reduces organic debris inputs from vegetation, leading to peat subsidence (Cahoon et al., 2003; Chambers et al., 2019). Subsidence lowers microtopography, extends seawater residence time, and promotes hypoxic conditions that can progress to anoxia. In our study, soil was the most affected carbon pool compared with total plant biomass. At the conserved site, SOC reached its maximum concentration in surface layers and progressively decreased with depth, whereas at the degraded site

the opposite pattern was observed, with reduced values at the surface and higher values at depth (Figure 4). This reversal in SOC distribution likely reflects the limited incorporation of organic residues from roots and leaf litter over more than a decade without natural regeneration. According to Jupin et al. (2024), inputs of autochthonous organic residues allow mangroves in the TLFFPA to maintain some of the highest sedimentary carbon burial rates recorded in Mexico. The absence of these inputs contributes to SOC losses by generating an imbalance between carbon sequestration and carbon release. In hurricane-impacted mangroves, this imbalance can be exacerbated by peat collapse (Cahoon et al., 2003; Chambers et al., 2019) and by increases in soil CO₂ and CH₄ fluxes under prolonged flooding, due to anaerobic conditions and intensified activity of methanogenic and sulfate-reducing microorganisms (Zou et al., 2025; Reed et al., 2025).

Overall, the marked reduction in TECS at the degraded site, together with altered SOC depth profiles and strongly reducing, hypersaline conditions, highlights the long-lasting effects of combined drought and hurricane impacts on mangrove carbon storage and the need for active intervention to reverse these trajectories.

4.2 Restoration of mangroves for carbon recovery

Recent studies indicate that assisted restoration can require up to 20 years to recover between 71% and 73% of ecosystem biomass and total carbon (Bourgeois et al., 2024). Despite the degree of degradation caused by hurricanes in the TLFFPA, we documented a recovery of 83% of the total ecosystem carbon stock at the restored



site ($286 \pm 32.6 \text{ Mg C ha}^{-1}$). The average TECS of the conserved site served as the reference for this estimate. The carbon storage capacity achieved at the restored site was slightly lower than the range reported for natural *A. germinans* mangroves in the region ($321\text{--}383 \text{ Mg C ha}^{-1}$; Hernández-Nava et al., 2022). For the different carbon pools, total tree biomass at the restored site reached 44% of conserved-site values after 14 years (Figure 5), whereas SOC (Mg C ha^{-1}) showed levels similar to those of the undisturbed ecosystem. These results support the hypothesis that hydrological rehabilitation (HR), when needed, enhances SOC storage within mangrove restoration projects.

Hydrological conditions are determinant for forest structure and vegetation health, as they regulate key factors such as salinity and nutrient availability (Flores-Verdugo et al., 2007). In this sense, hydrological rehabilitation at the restored site—through the clearing of natural channels and excavation of artificial ones—improved pore-water conditions to within the tolerance ranges of *Avicennia germinans* and *Rhizophora mangle*. Within 1 year, the restored hydrological regime reduced pore-water salinity, creating favorable conditions for regeneration, as reported in other studies (Garcés Ordóñez et al., 2021). Salinity continued to decline over the next 5 years and remained consistently low 14 years later, as shown by 2019 measurements (Supplementary Figure S4; Figure 3). These results demonstrate the long-term effectiveness of well-designed hydrological rehabilitation in sustaining mangrove hydrology.

In response to hydrological rehabilitation, the vegetation at the restored site developed forest attributes (such as basal area and height) characteristic of border-type mangroves dominated by *A. germinans*. At the regional level, forest structure in the TLFFPA is mainly composed of riparian *A. germinans* mangroves (50%), followed by border-type mangroves (38%) (Agraz Hernández et al., 2015; therefore, it is reasonable to assume that the restored site has reached an intermediate level of structural development. In addition, the low mortality rates and almost 39 years of vegetation dynamics reconstructed through NDVI show a sustained recovery,

with values similar to those recorded under pristine conditions in 1984. These vegetation index values reflect patterns of productivity and photosynthetic activity typical of healthy stands (Purwanto and Eviliyanto, 2022).

The increase in redox potential toward more oxygenated conditions observed at the restored site also appears to have favored SOC recovery, as indicated by the positive relationship between both variables (Supplementary Figure S5). HR actions restore water flow and reduce prolonged flooding, thereby improving oxygen availability in the soil and decreasing the concentration of reduced toxic compounds such as sulfide, Mn^{2+} , and ammonium (Pérez-Ceballos et al., 2020; López-Portillo et al., 2021). By mitigating this stress, roots can increase their development, which is essential for carbon sequestration because they constitute the main source of SOC (Zhang et al., 2021). In turn, greater oxygen availability favors the formation of iron oxyhydroxides, which participate in the stabilization of soil organic matter through chelation and co-precipitation processes (Yu et al., 2021). Finally, reconnection of the mangrove with tidal flow restores the deposition of sediments and terrigenous minerals, elements that enhance carbon burial (Jiménez et al., 2021; Jupin et al., 2024).

Altogether, these results indicate that hydrological rehabilitation and associated community-based restoration actions can recover most of the ecosystem carbon stocks lost after hurricane impacts, particularly in the soil pool, within approximately one to two decades. At the same time, the slower recovery of tree biomass and structural complexity suggests that full restoration of mangrove function and resilience may require longer time frames, underscoring the importance of continued monitoring and adaptive management.

In regions such as the TLFFPA, where more frequent droughts and hurricanes are expected, these results suggest that hydrological rehabilitation and community-based mangrove restoration can serve as robust nature-based solutions, supporting national climate commitments and blue-carbon initiatives while providing co-benefits for local livelihoods.

5 Conclusion

The Laguna de Términos region is highly susceptible to tropical cyclones, and coastal ecosystems such as mangroves can be severely affected by these hydrometeorological events. The extreme events of 1995 caused extensive mortality and the loss of natural regeneration capacity in large mangrove areas. This study demonstrates that well-planned mangrove restoration incorporating hydrological rehabilitation can achieve substantial recovery of carbon storage and ecosystem functioning within relatively short to medium timeframes. Fourteen years after intervention, total ecosystem carbon stock (TECS) at the restored site had recovered to 83% of the reference level. Hydrological rehabilitation improved interstitial water conditions, reduced salinity, and increased redox potential, favoring vegetation productivity and soil carbon stabilization. These results highlight ecological restoration as an effective strategy to enhance carbon storage, contribute to climate change mitigation, and conserve ecosystem services in vulnerable coastal areas.

Data availability statement

The raw data supporting the conclusions of this article will be made available by the authors, without undue reservation.

Author contributions

JC: Conceptualization, Visualization, Writing – review & editing, Investigation, Methodology, Formal analysis, Validation, Writing – original draft, Data curation. JG: Supervision, Conceptualization, Methodology, Writing – review & editing. JO: Writing – review & editing. MG: Writing – review & editing. AR: Writing – review & editing. RP: Methodology, Supervision, Writing – review & editing, Conceptualization. CA: Funding acquisition, Project administration, Supervision, Writing – review & editing, Methodology, Conceptualization.

Funding

The author(s) declared that financial support was received for this work and/or its publication. Laboratory facilities and logistical support for sample collection and analysis were provided by the Coastal Wetlands Laboratory and the EPOMEX Institute at the *Universidad Autónoma de Campeche*, Mexico. The Federal Electricity Commission (*Comisión Federal de Electricidad*, CFE) provided funding for the restoration as an environmental compensation measure for land-use change associated with the installation of power transmission towers. The *Universidad Autónoma de Campeche* covered the publication costs of the manuscript to enable its dissemination in open access.

Acknowledgments

This research is part of JCCB's doctoral thesis, conducted at the *Universidad Autónoma Metropolitana* (UAM, Mexico), thanks to the financial support of scholarships granted by the *Secretaría de Ciencias, Humanidades, Tecnología e Innovación* (SECIHTI) (Number Assigned to the Student: 926434) and the *Universidad Autónoma de Campeche* (UACAM, Mexico), in collaboration with the *French Global Environment Facility* (FFEM). We would like to thank Jordán Reyes and Adriana Gregorio for their valuable assistance during fieldwork and laboratory analysis. We also express our gratitude PhD. Rodolfo Enrique del Río Rodríguez for contributed to improving this manuscript.

Conflict of interest

The authors declared that this work was conducted in the absence of any commercial or financial relationships that could be construed as a potential conflict of interest.

Generative AI statement

The author(s) declared that generative AI was not used in the creation of this manuscript.

Any alternative text (alt text) provided alongside figures in this article has been generated by Frontiers with the support of artificial intelligence and reasonable efforts have been made to ensure accuracy, including review by the authors wherever possible. If you identify any issues, please contact us.

Publisher's note

All claims expressed in this article are solely those of the authors and do not necessarily represent those of their affiliated organizations, or those of the publisher, the editors and the reviewers. Any product that may be evaluated in this article, or claim that may be made by its manufacturer, is not guaranteed or endorsed by the publisher.

Supplementary material

The Supplementary Material for this article can be found online at: <https://www.frontiersin.org/articles/10.3389/fmars.2025.1722651/full#supplementary-material>

SUPPLEMENTARY FIGURE 1

Chronology and classification of hydrometeorological events in the Atlantic Ocean, showing only cyclones that made landfall on the continental territory of de Southeast México

SUPPLEMENTARY FIGURE 2

Tracking map of tropical cyclones Opal (a) and Roxanne (b) and in the Gulf of Mexico and the Yucatán Peninsula in 1995. Adapted from the National Oceanic and Atmospheric Administration (NOAA) interactive historical hurricane tracking platform. Parts of these two tropical cyclones, including their development from tropical depression to storm and hurricane, categorized by intensity based on the Saffir-Simpson Scale, a system for classifying tropical cyclones based on wind speed (Categories 1–5).

SUPPLEMENTARY FIGURE 3

Aerial image of the mangrove site classified as a degraded area within the Flora and Fauna Protection Area Laguna de Términos, Campeche, Mexico. The photograph shows extensive canopy loss and stands of dead trees, illustrating severe mangrove dieback and the degraded condition of the ecosystem.

SUPPLEMENTARY FIGURE 4

Annual pore-water salinity trends at a restored mangrove site within the Términos Lagoon Flora and Fauna Protection Area (Campeche State, Mexico) from 2005 to 2010. Data from 2005 were collected prior to restoration, whereas values from 2006 onward reflect restoration effects. Vertical lines represent the standard error of the mean. Different capital letters (A, B, C) denote statistically significant differences between years based on a *post-hoc* analysis.

SUPPLEMENTARY FIGURE 5

Linear regressions between soil organic carbon content and redox potential in *Avicennia germinans* mangroves within the Términos Lagoon Flora and Fauna Protection Area (Campeche State, Mexico). The data correspond to point measurements taken in 2019 at a degraded site, a reference site, and a restored site.

References

- Agraz Hernández, C., Andrieu, J., Cormier-Salem, M. C., Gabrié, C., Macera, L., and Proserpi, J. (2024). *Guide méthodologique pour la restauration des mangroves*. (French Global Environment Facility (FFEM). Available online at: <https://hal.science/hal-04567145v1/document> (Accessed March 15, 2025).
- Agraz-Hernández, C. M., Chan-Keb, C. A., Muñoz-Salazar, R., Pérez-Balan, R. A., Osti-Sáenz, J., Gutiérrez-Alcántara, E. J., et al. (2020). Relationship between blue carbon and methane and the hydrochemistry of mangroves in southeast Mexico. *Appl. Ecol. Environ. Res.* 18, 1091–1106. doi: 10.15666/aeer/1801_10911106
- Agraz-Hernández, C. M., Chan-Keb, C. A., Muñoz-Salazar, R., Pérez-Balan, R. A., Vanegas, G. P., Manzanilla, H. G., et al. (2022). Pore water chemical variability and its effect on phenological production in three mangrove species under drought conditions in southeastern Mexico. *Diversity* 14, 668. doi: 10.3390/d14080668
- Agraz Hernández, C. M., Houndjino, E., Reyes Castellanos, J. E., Chan Keb, C. A., Osti Sáenz, J., Chávez Barrera, J. C., et al. (2025). Hydrological repair and invasive grass removal restore *Rhizophora racemosa* mangrove communities in West Africa. *Restor. Ecol.* 33 (7), e70084. doi: 10.1111/rec.70084
- Agraz Hernández, C., Sáenz, J., Keb, C., Martínez, V., Acosta-Velázquez, J., Domínguez, S., et al. (2015). “Grado de conservación del ecosistema de mangle en la Laguna de Términos, Campeche: Propuesta de políticas ambientales y acciones de restauración,” in *Aspectos socioambientales de la región de la Laguna de Términos*, 1st ed. Eds. J. Ramos Miranda and G. J. Villalobos Zapata (Campeche, México: Universidad Autónoma de Campeche), 210.
- Alongi, D. M. (2020). Global significance of mangrove blue carbon in climate change mitigation. *Sci* 2, 67. doi: 10.3390/sci2030067
- Amaral, C., Poulter, B., Lagomasino, D., Fatoyinbo, T., Taillie, P., Lizcano, G., et al. (2023). Drivers of mangrove vulnerability and resilience to tropical cyclones in the North Atlantic Basin. *Sci. Total Environ.* 898, 165413. doi: 10.1016/j.scitotenv.2023.165413
- Asbridge, E. F., Bartolo, R., Finlayson, C. M., Lucas, R. M., Rogers, K., Woodroffe, C. D., et al. (2019). Assessing the distribution and drivers of mangrove dieback in Kakadu National Park, northern Australia. *Estuarine Coast. Shelf Sci.* 228, 106353. doi: 10.1016/j.ecss.2019.106353
- Bourgeois, C. F., MacKenzie, R. A., Sharma, S., Bhomia, R. K., Johnson, N. G., Rovai, A. S., et al. (2024). Four decades of data indicate that planted mangroves stored up to 75% of the carbon stocks found in intact mature stands. *Sci. Adv.* 10, eadk5430. doi: 10.1126/sciadv.adk5430
- Bunting, P., Rosenqvist, A., Lucas, R. M., Rebelo, L. M., Hilarides, L., Thomas, N., et al. (2018). The global mangrove watch—A new 2010 global baseline of mangrove extent. *Remote Sens.* 10, 1669. doi: 10.3390/rs10101669
- Cahoon, D. R., Hensel, P., Rybczyk, J., McKee, K. L., Proffitt, C. E., and Perez, B. C. (2003). Mass tree mortality leads to mangrove peat collapse at Bay Islands, Honduras after Hurricane Mitch: Hurricane-induced mangrove peat collapse. *J. Ecol.* 91, 1093–1105. doi: 10.1046/j.1365-2745.2003.00841.x
- Chambers, L. G., Steinhilber, H. E., and Breithaupt, J. L. (2019). Toward a mechanistic understanding of “peat collapse” and its potential contribution to coastal wetland loss. *Ecology* 100, e02720. doi: 10.1002/ecy.2720
- Chávez Barrera, J. C., Gallardo Lancho, J. F., Puschendorf, R., and Agraz Hernández, C. M. (2025). Loss and early recovery of biomass and soil organic carbon in restored mangroves after *Paspalum vaginatum* invasion in West Africa. *Resources* 14, 122. doi: 10.3390/resources14080122
- Chen, J., Per, CheckGivenNames/>Jouml;nsson, Tamura, M., Gu, Z., Matsushita, B., et al. (2004). A simple method for reconstructing a high-quality NDVI time-series data set based on the Savitzky–Golay filter. *Remote Sens. Environ.* 91, 332–344. doi: 10.1016/j.rse.2004.03.014
- Coumou, D., and Rahmstorf, S. (2012). A decade of weather extremes. *Nat. Clim. Change* 2, 491–496. doi: 10.1038/nclimate1452
- Day, J. W., Conner, W. H., Ley-Lou, F., Day, R. H., and Navarro, A. M. (1987). The productivity and composition of mangrove forests, Laguna de Términos, Mexico. *Aquat. Bot.* 27, 267–284. doi: 10.1016/0304-3770(87)90046-5
- De La Barreda, B., Metcalfe, S. E., and Boyd, D. S. (2020). Precipitation regionalization, anomalies and drought occurrence in the Yucatan Peninsula, Mexico. *International Journal of Climatology* 40, 4541–4555. doi: 10.1002/joc.6474
- Donato, D. C., Kauffman, J. B., Murdiyoso, D., Kurnianto, S., Stidham, M., and Kanninen, M. (2011). Mangroves among the most carbon-rich forests in the tropics. *Nat. Geosci* 4, 293–297. doi: 10.1038/ngeo1123
- Duncan, C., Primavera, J. H., Hill, N. A. O., Wodehouse, D. C. J., and Koldewey, H. J. (2022). Potential for return on investment in rehabilitation-oriented blue carbon projects: Accounting methodologies and project strategies. *Front. For. Glob. Change* 4, doi: 10.3389/ffgc.2021.775341
- Echeverría-Ávila, S., Pérez-Ceballos, R., Zaldivar-Jimenez, M., Canales-Delgado, J., Brito-Pérez, R., Merino-Ibarra, M., et al. (2019). Regeneración natural de sitios de manglar degradado en respuesta a la restauración hidrológica. *Madera y Bosques* 25 (1), e2511754. doi: 10.21829/myb.2019.2511754
- Flores-Verdugo, F., Moreno-Casasola, P., Agraz-Hernández, C. M., López-Rosas, H., Benítez-Pardo, D., Travieso-Bello, A. C., et al. (2007). La topografía y el hidropérido: dos factores que condicionan la restauración de los humedales costeros. *Bot. Sci.* 33–47. doi: 10.17129/botsci.1755
- Fromard, F., Puig, H., Mougin, E., Marty, G., Betoulle, J. L., and Cadamuro, L. (1998). Structure, above-ground biomass and dynamics of mangrove ecosystems: new data from French Guiana. *Oecologia* 115, 39–53. doi: 10.1007/s004420050489
- Garcés Ordóñez, O., Rodríguez, A., Espinosa Díaz, L., Escobar Toledo, F., and DelValle Borrero, D. (2021). Respuesta a corto plazo de parámetros fisicoquímicos del agua a la rehabilitación hidrológica de caños en manglares de Cispata, Caribe Colombiano. *Bol. Investig. Mar. Costeras* 50, 151–160. doi: 10.25268/bimc.invemar.2021.50.2.1106
- Gatt, Y. M., Walton, R. W., Andradi-Brown, D. A., Spalding, M. D., Acosta-Velázquez, J., Adame, M. F., et al. (2024). The Mangrove Restoration Tracker Tool: Meeting local practitioner needs and tracking progress toward global targets. *One Earth* 7, 2072–2085.
- Gerona-Daga, M. E. B., and Salmo, S. G. (2022). A systematic review of mangrove restoration studies in Southeast Asia: Challenges and opportunities for the United Nation’s Decade on Ecosystem Restoration. *Front. Mar. Sci.* 9. doi: 10.3389/fmars.2022.987737
- Getzner, M., and Islam, M. S. (2020). Ecosystem services of mangrove forests: results of a meta-analysis of economic values. *IJERPH* 17, 5830. doi: 10.3390/ijerph1716583
- Grenz, C., Fichez, R., Silva, C.Á., Benítez, L. C., Conan, P., Esparza, A. C. R., et al. (2017). Benthic ecology of tropical coastal lagoons: Environmental changes over the last decades in the Términos Lagoon, Mexico. *Comptes Rendus. Géoscience* 349, 319–329. doi: 10.1016/j.crte.2017.09.016
- Griffiths, L. N., and Mitsch, W. J. (2021). Estimating the effects of a hurricane on carbon storage in mangrove wetlands in southwest florida. *Plants* 10, 1749. doi: 10.3390/plants10081749
- Grimm, K. E., Archibald, J. L., Axelsson, E. P., and Grady, K. C. (2023). Follow the money: Understanding the Latin America and Caribbean mangrove restoration funding landscape to assist organizations and funders in improved social-ecological outcomes. *Conserv. Sci. Prac.* 5, e12815. doi: 10.1111/csp.2.12815
- Hai, N. T., Dell, B., Phuong, V. T., and Harper, R. J. (2020). Towards a more robust approach for the restoration of mangroves in Vietnam. *Annals of Forest Science* 77, 18. doi: 10.1007/s13595-020-0921-0
- Hernández-Nava, J., Pascual-Barrera, A. E., Zaldivar-Jiménez, A., and Pérez-Ceballos, R. (2022). Estructura y secuestración de carbono en manglares urbanos, fundamentos para su conservación en Isla del Carmen, Campeche, México. *Bot. Sci.* 100, 899–911. doi: 10.17129/botsci.3048
- Jiménez, L. C. Z., Queiroz, H. M., Otero, X. L., Nóbrega, G. N., and Ferreira, T. O. (2021). Soil organic matter responses to mangrove restoration: a replanting experience in northeast Brazil. *IJERPH* 18, 8981. doi: 10.3390/ijerph18178981
- Jupin, J. L. J., Ruiz-Fernández, A. C., Sifeddine, A., Mendez-Millan, M., Sanchez-Cabeza, J. A., Pérez-Bernal, L. H., et al. (2024). Terrestrial inputs boost organic carbon accumulation in Mexican mangroves. *Sci. Total Environ.* 940, 173440. doi: 10.1016/j.scitotenv.2024.173440
- Kauffman, K., and Donato, D. (2012). *Protocols for the measurement, monitoring and reporting of structure, biomass and carbon stocks in mangrove forests* (Bogor, Indonesia: Center for International Forestry Research (CIFOR). doi: 10.17528/cifor/003749
- Komiyama, A., Ong, J. E., and Pongpam, S. (2008). Allometry, biomass, and productivity of mangrove forests: A review. *Aquat. Bot.* 89, 128–137. doi: 10.1016/j.aquabot.2007.12.006
- Krauss, K. W., Lovelock, C. E., McKee, K. L., López-Hoffman, L., Ewe, S. M. L., and Sousa, W. P. (2008). Environmental drivers in mangrove establishment and early development: A review. *Aquat. Bot.* 89, 105–127. doi: 10.1016/j.aquabot.2007.12.014
- Laboratorio de Humedales Costeros. (2025). Beneficios sociales. Available online at: <https://www.humedalescosterospomex.com/ES/beneficiosociales.html> (Accessed October 15, 2025).
- Lagomasino, D., Fatoyinbo, T., Castañeda-Moya, E., Cook, B. D., Montesano, P. M., Neigh, C. S. R., et al. (2021). Storm surge and ponding explain mangrove dieback in southwest Florida following Hurricane Irma. *Nat. Commun.* 12, 4003. doi: 10.1038/s41467-021-24253-y
- Landsea, C. W., Bell, G. D., Gray, W. M., and Goldenberg, S. B. (1998). The extremely active 1995 Atlantic hurricane season: environmental conditions and verification of seasonal forecasts. *Monthly Weather Rev.* 126, 1174–1193. doi: 10.1175/1520-0493(1998)126<1174:TEAAHS>2.0.CO;2
- Lewis, R. R. (2005). Ecological engineering for successful management and restoration of mangrove forests. *Ecol. Eng.* 24, 403–418. doi: 10.1016/j.ecoleng.2004.10.003
- Lovelock, C. E., Barbier, E., and Duarte, C. M. (2022). Tackling the mangrove restoration challenge. *PLoS Biology* 20, e3001836. doi: 10.1371/journal.pbio.3001836

- López-Portillo, J., Zaldivar-Jiménez, A., Lara-Domínguez, A. L., Pérez-Ceballos, R., Bravo-Mendoza, M., Alvarez, N. N., et al. (2021). "Hydrological rehabilitation and sediment elevation as strategies to restore mangroves in terrigenous and calcareous environments in Mexico," in *Geophysical monograph series*. Eds. K. W. Krauss, Z. Zhu and C. L. Stagg (Hoboken, NJ: Wiley), 173–190. doi: 10.1002/9781119639305.ch9
- Macías Samano, J. E., Agraz Hernández, C. M., and Villa Castillo, J. (2025). Sanidad o salud forestal en México: estudios comparativos en tres ecosistemas protegidos. *RMCF* 16. doi: 10.29298/rmcf.v16i90.1543
- Owuor, M., Santos, T. M. T., Otieno, P., Mazzuco, A. C. A., Iheaturu, C., and Bernardino, A. F. (2024). Flow of mangrove ecosystem services to coastal communities in the Brazilian Amazon. *Front. Environ. Sci.* 12. doi: 10.3389/fenvs.2024.1329006
- Palacio Prieto, J. L., Ortiz Pérez, M. A., and Garrido Pérez, A. (1999). Cambios morfológicos costeros en Isla del Carmen, Campeche, por el paso del huracán "Roxanne". *Investigaciones Geográficas* 40, 48–57.
- Peneva-Reed, E. I., Krauss, K. W., Bullock, E. L., Zhu, Z., Woltz, V. L., Drexler, J. Z., et al. (2021). Carbon stock losses and recovery observed for a mangrove ecosystem following a major hurricane in Southwest Florida. *Estuarine Coast. Shelf Sci.* 248, 106750. doi: 10.1016/j.ecss.2020.106750
- Pereira Silva, B., Saballo, H. M., Lobo, A. K. M., and Neto, M. C. L. (2023). The plasticity of the photosynthetic apparatus and antioxidant responses are critical for the dispersion of *Rhizophora mangle* along a salinity gradient. *Aquatic Botany* 185, 103609. doi: 10.1016/j.aquabot.2022.103609
- Reed, D., Chavez, S., Castañeda-Moya, E., Oberbauer, S. F., Troxler, T., Malone, S., et al. (2025). Resilience to hurricanes is high in mangrove blue carbon forests. *Global Change Biology* 31, e70124. doi: 10.1111/gcb.70124
- Pérez-Ceballos, R., Zaldivar-Jiménez, A., Canales-Delgadillo, J., López-Adame, H., López-Portillo, J., and Merino-Ibarra, M. (2020). Determining hydrological flow paths to enhance restoration in impaired mangrove wetlands. *PLoS One* 15, e0227665. doi: 10.1371/journal.pone.0227665
- Rivera-Monroy, V. H., Farfán, L. M., Brito-Castillo, L., Cortés-Ramos, J., González-Rodríguez, E., D'Sa, E. J., et al. (2020). Tropical cyclone landfall frequency and large-scale environmental impacts along karstic coastal regions (Yucatán Peninsula, Mexico). *Appl. Sci.* 10, 5815. doi: 10.3390/app10175815
- Tran, T. V., Reef, R., and Zhu, X. (2022). A review of spectral indices for mangrove remote sensing. *Remote Sens.* 14, 4868. doi: 10.3390/rs14194868
- Troche-Souza, C., Villeda-Chávez, E., Vázquez-Balderas, B., Velázquez-Salazar, S., Vázquez-Morán, V. H., Rosas-Aceves, O. G., et al. (2025). Spatial distribution of mangrove forest carbon stocks in marismas nacionales, Mexico: contributions to climate change adaptation and mitigation. *Forests* 16, 1224. doi: 10.3390/f16081224
- Velázquez-Salazar, S., Rodríguez-Zúñiga, M. T., Alcántara-Maya, J. A., Villeda-Chávez, E., Valderrama-Landeros, L., Troche-Souza, C., et al. (2020). "Manglares de México," in *Actualización y análisis de los datos 2020* (Comisión Nacional para el Conocimiento y Uso de la Biodiversidad, México CDMX), 168.
- Winarso, G., Rosid, M. S., Kamal, M., Asriningrum, W., Margules, C., and Supriatna, J. (2023). Comparison of mangrove Index (MI) and Normalized Difference Vegetation Index (NDVI) for the detection of degraded mangroves in Alas Purwo Banyuwangi and Segara Anakan Cilacap, Indonesia. *Ecol. Eng.* 197, 107119. doi: 10.1016/j.ecoleng.2023.107119
- Xiong, L., Lagomasino, D., Charles, S. P., Castañeda-Moya, E., Cook, B. D., Redwine, J., et al. (2022). Quantifying mangrove canopy regrowth and recovery after Hurricane Irma with large-scale repeat airborne lidar in the Florida Everglades. *Int. J. Appl. Earth Observation Geoinformation* 114, 103031. doi: 10.1016/j.jag.2022.103031
- Yu, C., Xie, S., Song, Z., Xia, S., and Åström, M. E. (2021). Biogeochemical cycling of iron (hydr)-oxides and its impact on organic carbon turnover in coastal wetlands: A global synthesis and perspective. *Earth-Science Rev.* 218, 103658. doi: 10.1016/j.earscirev.2021.103658
- Zhang, Y., Xiao, L., Guan, D., Chen, Y., Motelica-Heino, M., Peng, Y., et al. (2021). The role of mangrove fine root production and decomposition on soil organic carbon component ratios. *Ecol. Indic.* 125, 107525. doi: 10.1016/j.ecolind.2021.107525
- Zou, H., Zhu, J., Tian, Z., Chen, Z., Xue, Z., and Li, W. (2025). Response mechanism of carbon fluxes in restored and natural mangrove ecosystems under the effects of storm surges. *Forests* 16, 1115. doi: 10.3390/f16071115